Citation: Molecular Therapy — Methods & Clinical Development (2016) **3,** 16012; doi:10.1038/mtm.2016.12
Official journal of the American Society of Gene & Cell Therapy

www.nature.com/mtm

ARTICLE

All-in-one processing of heterogeneous human cell grafts for gene and cell therapy

Ekaterina Y Lukianova-Hleb[1,2], Eric S Yvon[3], Elizabeth J Shpall[3] and Dmitri O Lapotko[1,2]

Authors dedicate this work to Dr. Leslie Huye who took part in the early development of this cancer-aimed technology. Destroyed by cancer, she was never defeated.

Current cell processing technologies for gene and cell therapies are often slow, expensive, labor intensive and are compromised by high cell losses and poor selectivity thus limiting the efficacy and availability of clinical cell therapies. We employ cell-specific on-demand mechanical intracellular impact from laser pulse-activated plasmonic nanobubbles (PNB) to process heterogeneous human cell grafts *ex vivo* with dual simultaneous functionality, the high cell type specificity, efficacy and processing rate for transfection of target CD3+ cells and elimination of subsets of unwanted CD25+ cells. The developed bulk flow PNB system selectively processed human cells at a rate of up to 100 million cell/minute, providing simultaneous transfection of CD3+ cells with the therapeutic gene (FKBP12(V36)-p30Caspase9) with the efficacy of 77% and viability 95% (versus 12 and 60%, respectively, for standard electroporation) and elimination of CD25+ cells with 99% efficacy. PNB flow technology can unite and replace several methodologies in an all-in-one universal *ex vivo* simultaneous procedure to precisely and rapidly prepare a cell graft for therapy. PNB's can process various cell systems including cord blood, stem cells, and bone marrow.

Molecular Therapy — Methods & Clinical Development (2016) **3**, 16012; doi:10.1038/mtm.2016.12; published online 16 March 2016

INTRODUCTION

Most cell and gene therapies that have shown promise against human diseases including cancer require *ex vivo* processing of human cell grafts. This processing eliminates unwanted cells from a heterogeneous suspension and genetically modifies (transfects) specific cell subsets to increase their therapeutic efficacy. Ideally both elimination and transfection should be highly efficient, selective, and fast with the minimal losses of important cells. Existing methods, however, do not support simultaneous elimination and transfection in heterogeneous cell systems.[1–20] Cell destruction (elimination, separation) uses filtering, centrifuging, fluorescent-activated flow sorting, and magnetic, and adsorbent removal of target cells. The best results were achieved with target-specific antibodies conjugated to either magnetic beads or biotin to bind to the target cells and then to pass through columns to select the target cells.[1–12] When applied to human grafts, the limitations of immunotargeting are in the incomplete removal of unwanted cells or the excessive removal of important immune cells,[1,8–12] as well as the lack of selectivity due to unavoidable nonspecific binding of antibodies to nontarget cells. Cell transfection is similarly limited. Three major transfection approaches deliver plasmids with viral,[13–15] nonviral using plasmid carriers,[15–20] and nonviral using external energy[15,18,21–45] methods. While viruses offer greater efficacy of gene transfer, nonviral methods provide better safety and are usually less immunogenic. Carrier-based approaches use liposomes, dendrimers, polyplexes, polyethyleneimine, and other nanoparticles. Of these methods, lipofection (liposomes as carriers) is widespread.[18,20,31–36] Use of plasmid carriers improves the efficacy and safety of gene transfer,[17,19,37–42] but the selectivity of such methods in heterogeneous cell systems is limited by the nonspecific uptake of carriers by nontarget cells. External energy-based methods use sono-, electro- and opto-poration of cells,[18,22–30,42] of which electroporation/nucleofection is most widely used,[18,24,42] but delivers poor selectivity and cell viability. As a result, current cell processing is often slow, expensive, labor intensive and is compromised by high cell losses and poor selectivity thus limiting the efficacy and availability of cell therapies, especially in clinic.

Here, we report a novel universal technology for *ex vivo* bulk processing of heterogeneous cell systems with dual simultaneous functionality, single cell type specificity, high efficacy and processing rate, and low toxicity: (i) elimination of subsets of unwanted cells (Figure 1a), (ii) transfection of target cells (Figure 1b). This goal was achieved using our newly developed class of cellular nonstationary nano-events, called plasmonic nanobubbles (PNBs).[46–49] A PNB is not a particle but a transient nanosecond intracellular event, a vapor nanobubble that is generated around a gold nanoparticle (GNP) cluster when it absorbs a short laser pulse, converts its energy into heat and evaporates its liquid environment in a nano-explosive manner. We recently demonstrated the high target cell specificity of PNBs (10-fold higher than for targeted nanoparticles),[48–50] the trans-membrane injection of molecular cargo to,[51–54] and the immediate mechanical destruction (elimination) of, specific target

[1]Department of BioSciences, Rice University, Houston, Texas, USA; [2]Current address: Masimo Corporation, Irvine, California, USA; [3]Department of Stem Cell Transplantation, The University of Texas MD Anderson Cancer Center, Houston, Texas, USA Correspondence: Dmitri O Lapotko (dmitrilapotko@yahoo.com)
Received 5 December 2015; accepted 28 January 2016

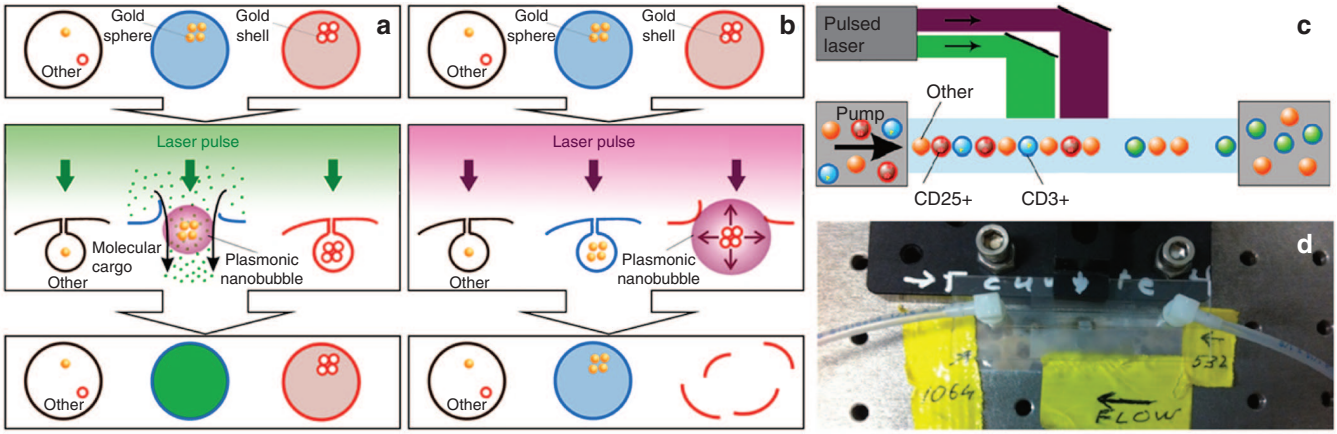

Figure 1 Principle of simultaneous plasmonic nanobubble (PNB) treatment with PNBs of different sizes. (**a**) selective transfection of CD3+ cells (blue) under excitation of 532 nm laser pulse, (**b**) selective destruction of CD25+ cells (brown) under excitation of 1,064 nm laser pulse. (**c**) Diagram of the flow system with the two spatially-separated laser beams, 532 and 1,064 nm, aligned to expose flowing cells in the cuvette, and (**d**) photo of the flow cuvette with the transparent channel of 5 × 0.8 mm cross-section installed for the laser treatment.

cells[54–58] and, most importantly, an ability to simultaneously generate cell type-specific PNBs with different functions.[54] This dual functionality of PNBs, either injection of the external cargo or cell destruction, is determined by the maximal size of the PNB, which, in turn, is determined by the GNP and laser pulse properties.[46,47] Here, we apply this dual simultaneous functionality and high target cell specificity of PNBs to engineer human cell graft by simultaneously transfecting CD3+ blood cells with the therapeutic gene and eliminating unwanted regulatory CD25+ blood cells in one high-throughput bulk treatment that delivers up to 100 million cells per minute and minimizes the cell losses and processing time in all-in-one simple and safe procedure.

RESULTS

Generation of cell type-specific PNBs

To establish the mechanism for dual PNB functionality with the therapeutic gene, we studied the generation of PNBs in human CD3+ and CD25+ cells under identical optical treatment with single laser pulses in individual cells. To achieve the desired PNB size and selectivity (which supports cell type-specific functionality of PNB), two cell sub-sets were targeted with two different GNP types each of which had different PNB generation efficacy. To generate relatively small sublethal PNBs in CD3+ cells for gene transfection, we used 60 nm solid gold spheres covalently conjugated to anti-CD3 antibody (NSP60-CD3 conjugates) with the optical absorption maximum close to 532 nm. To generate large lethal PNBs in CD25+ cells for their elimination, we employed 240 nm solid silica-gold shells covalently conjugated to anti-CD25 antibody (NS240-CD25 conjugates) with the optical absorption maximum close to 1,064 nm. After incubating each cell subset with gold conjugates for 1 hour, the maximal diameter of PNBs was measured in individual cells through the PNB lifetime (duration of PNB-specific optical time-responses) as a function of the fluence of the laser pulse at 532 nm in CD3+ cells and 1,064 nm in CD25+ cells (Figure 2a). The generation of PNBs in each individual cell was verified via the shape of the optical scattering time-responses (insets in Figure 2a), which produced PNB-specific dip-shaped signals. With these data, we determined the optimal laser pulse fluence for each laser wavelength: at 532 nm, the laser pulse induced sublethal PNBs in CD3+ cells for injection of plasmid, at 1,064 nm, the laser pulse induced the large lethal PNBs in CD25+ cells for their elimination. At both wavelengths, such PNBs were achieved at the safe levels of laser fluence of 60–65 mJ/cm^2.

Next, we measured the selectivity of PNB generation under identical treatment of both cell types with gold conjugates and laser pulses. We measured the PNB lifetime in individual cells as the cell population-averaged value as function of the laser wavelength for several combinations of the cell type and gold conjugates. Each measurement was obtained in response to a single pulse of 532 and 1,064 nm at the fluence of 65 mJ/cm^2 (Figure 2b). For all combinations of gold conjugates and laser pulses, only one, NSP60-CD3 and 532 nm pulse, resulted in PNBs of 95 ± 7 ns lifetime in CD3+ cells. In CD25+cells, the lethal PNBs of 298 ± 24 ns lifetime were achieved only with the combination NS240-CD25 and 1,064 nm pulse. Other combinations did not return significant PNBs. Thus, when the mixture of CD3+ and CD25+ cells was identically treated with both gold conjugates and two laser pulses of 532 nm and then 1,064 nm, cell subset-specific PNB sizes were selectively induced to support noninvasive injection of plasmid with small PNBs in CD3+ cells and elimination of CD25+ through their mechanical destruction with large lethal PNBs (Figure 2b). We next evaluated the feasibility of this gold-laser dual functionality of PNBs in human cells.

PNBs efficiently destroy CD25+ cells

We measured the efficacy of the destruction of CD25+ cells with PNBs in the bulk static laser treatment (a single pulse exposed many cells at a time) under the above-determined parameters of gold conjugates and laser pulses. Specifically, we measured the combination metric named effective cell viability (product of the viability and cell concentration, see the Methods section for details) as function of the laser pulse fluence 10 minutes after exposing many cells to a broad single 1,064 nm laser pulse. We compared the CD25+ effective cell viability level after their exposure to a single laser pulse to that measured before the exposure to the laser pulse (Figure 3c). Almost total (> 99% of the initial level of the effective cell viability) destruction of the CD25+ cells was achieved under the fluence of 65 mJ/cm^2 (as verified 10 minutes after laser treatment by measuring the cell concentration and viability and monitoring their product, the efficient cell viability), which corresponded to the lethal PNBs with the lifetime of 298 ± 24 ns (Figure 2a). In addition, visual comparison of the cells before (Figure 3a) and after (Figure 3b) the laser

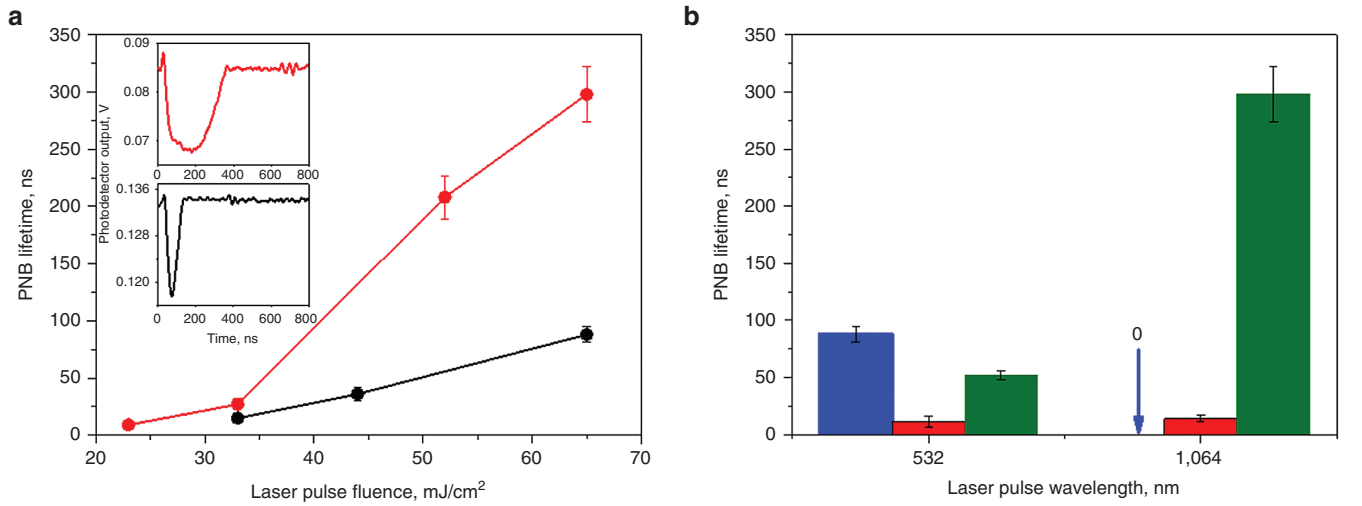

Figure 2 Cell type-specific generation of plasmonic nanobubbles (PNBs). (**a**) Plasmonic nanobubble (PNB) lifetime as function of the laser pulse fluence in CD25-positive (red) and CD3-positive (black) individual cells (CD25 cells were treated with NS240-CD25 gold conjugates and 1,064 nm laser pulse; CD3 cells were treated with NSP60-CD3 gold cinjugates and 532 nm laser pulse). Insets show typical time-responses of PNBs in CD25-positive (red) and CD3-positive (black) cells. (**b**) PNB lifetime in cells as a function of the laser pulse wavelength (laser pulse fluence 65 mJ/cm^2) and of the incubation conditions: blue—CD3-positive cells treated by NSP60-CD3 gold conjugates, red—CD3-positive cells treated by NS240-CD25 gold conjugates, green—CD25-positive cells treated by NS240-CD25 gold conjugates (50–100 cells were individually measured for each data point).

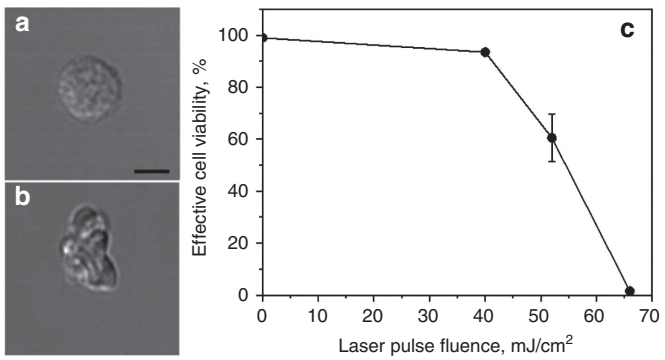

Figure 3 PNB-induced destruction of CD25-positive cells. Bright-filed image of CD25-positive cell before (**a**) and after (**b**) plasmonic nanobubble treatment with a single laser pulse (1,064 nm, 65 mJ/cm^2). (**c**) The effective viability of CD25-positive cells viability as a function of the laser pulse fluence in 10 minutes after cell processing. Scale bar: 5 µm.

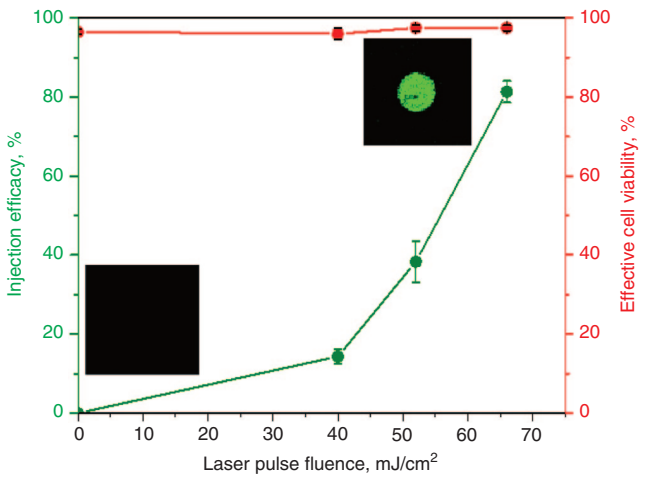

Figure 4 PNB-induced injection of molecular cargo to CD3-positive cells. Dependence of the Dextran injection efficacy (green) and the effective cell viability (red) of CD3-positive cells as function of the laser pulse fluence. Insert show the typical fluorescent images of the cells before (left) and after (right, top) the PNB treatment. The effective cell viability was measured 10 minutes after the PNB treatment.

pulse also confirmed the destruction of CD25+ cells. This destruction was caused by the mechanical disruptive impact of large intracellular PNBs (the mechanism studied by us in detail earlier[48,54–60]) and was verified with three techniques by comparing the cell viability, concentration, and image.

PBNs safely inject external cargo into CD3+ cells

We measured the safety and efficacy of injecting external molecular cargo into CD3+ cells using bulk static laser treatment by exposing many cells with a broad single laser pulse. We used the above-determined parameters of gold conjugates and laser pulses to generate small nonlethal PNBs. Green fluorescent Dextran (2 MDa weight) was used as a model cargo. Specifically, we measured the percentage of green-fluorescent CD3+ cells and their effective viability (Figure 4) as a function of the laser pulse fluence. The effective cell viability was measured before and 10 minutes after the laser treatment with a single 532 nm laser pulse to determine the percentage of survived cells relative to untreated cells. Observing green fluorescence after PNB treatment confirmed the cargo injection, as demonstrated in the visual comparison of the cells before (black inset Figure 4) and after (green inset Figure 4) the laser pulse. Generally, the injection efficacy increased with the laser fluence (which determines the maximal diameter of the PNB[47]). We achieved the high (>81 ± 3%) injection efficacy of the CD3+ cells under the fluence of 65 mJ/cm^2, which corresponded to the PNBs of 88 ± 7 ns lifetime (Figure 2a). The mechanical impact of PNB has induced the injection of extracellular Dextran. PNB has transiently perforated the cell membrane and injected the external molecules into the cytoplasm during its collapse.[53] Only small, relatively noninvasive PNBs were generated in this mode, making the injection noninvasive in the whole range of laser pulse fluences as we verified with two independent measurements of the cell concentration and viability (presented through their combination metric of the effective cell viability, Figure 2b).

PBNs transfect human T-cells with therapeutic genes

To analyze the safety and efficacy of PNB-induced transfection of CD3+ cells with the therapeutic gene FKBP12(V36)-p30Caspase9, we used PNBs to inject the plasmid pMSCV-F-del Casp9.IRES.GFP. The previous experiment was repeated in the static laser treatment mode, with the Dextran replaced by plasmid at various concentrations. We measured the transfection efficacy (percentage of green fluorescence-positive cells) as a function of the PNB lifetime (maximal size of the PNB), plasmid concentration and time after the PNB treatment (Figure 5). Many cells were simultaneously exposed to a single 532 nm broad laser pulse. As a reference control, we measured the level of fluorescence in cells identically exposed to plasmid but not to the laser pulse. Generation of PNBs was monitored through their time-responses as described above.

The transfection dynamics was monitored after a single laser pulse treatment at the plasmid concentration of 50 µg/ml and laser fluence of 65 mJ/cm^2 (corresponded to the PNB lifetime of 88 ± 7 ns). We observed stable onset of green fluorescence in most of the cells on day 3–4 only in PNB-treated CD3+ cells (Figure 5a, insets show the fluorescent images of the cells on the day 1 and 3).

We measured the influence of the plasmid concentration on the transfection efficacy under specific laser fluence of 65 mJ/cm^2 (corresponds to the PNB lifetime of 88 ± 7 ns) 72 hours after PNB generation in CD3+ cells (Figure 5b). Plasmid concentrations of 50 µg/ml and higher provided efficient transfection. We observed stable transfection of CD3+ cells with the therapeutic gene with the efficacy increasing up to 81 ± 4% with the PNB lifetime (Figure 5c) for the combination of plasmid concentration 50 µg/ml and post-laser irradiation time of 72–96 hours. PNB treatment was also safe for CD3+ cells (Figure 5c): the effective viability of transfected cells remained above 97% (relative to that of the untreated cells). In this study, the priority was given to achieve the combination of high transfection efficacy and sustained cell viability. These static experiments established the PNB mechanisms of transfection of CD3+ cells with the therapeutic gene and elimination of CD25+ cells. These mechanisms were next applied to the bulk flow all-in-one cell processing technology.

Flow bulk PNB treatment of the CD3+ and CD25+ cells

Finally, we tested the developed technology in its full mode, *i.e.*, the bulk flow dual-functional cell processing. The PNB technology has been prototyped to combine the high cell processing rate and single cell selectivity of the cell processing. We achieved these cell processing rate and selectivity by: (i) flowing the cell suspension through a wide optically transparent cuvette (ibidi µ-slides I Luer, Martinsried, Germany) with the cross-section around 5 mm^2, (ii) exposing cells to

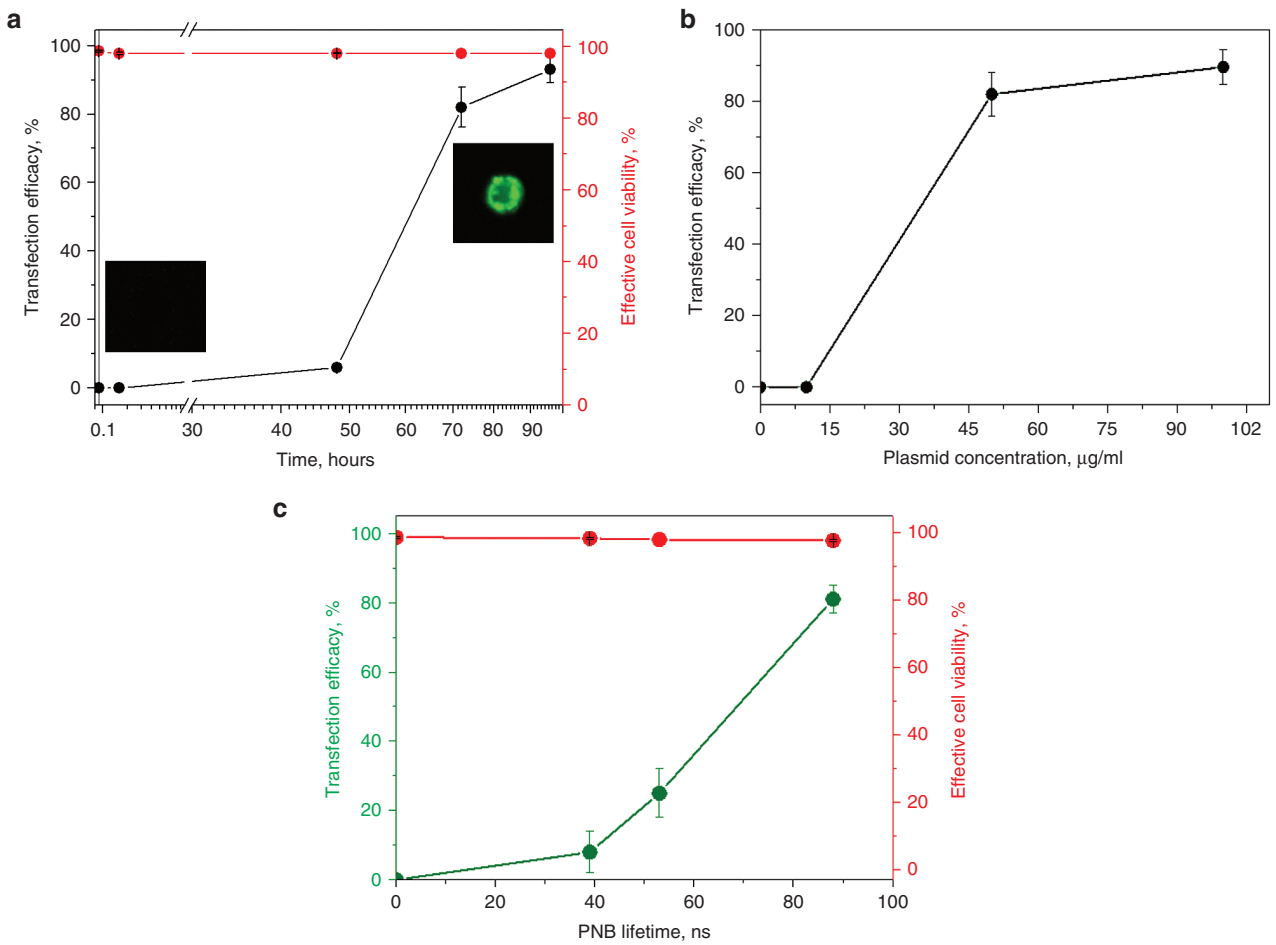

Figure 5 Transfection of CD3-positive cells with therapeutic gene. The transfection efficacy (percentage of green fluorescence-positive cells) of CD3-positive cells with the therapeutic gene FKBP12(V36)-p30Caspase9 as a function of: (**a**) time and the effective cell viability after the plasmonic nanobubble (PNB) generation (insets show typical fluorescent images of cells 24 (left corner) and 96 (right top corner) hours after the PNB generation), (**b**) plasmid concentration (72 hours after the PNB generation), and (**c**) PNB lifetime (green, measured 72 hours after the PNB generation), red: the effective cell viability of PNB-treated cells 72 hours after the treatment (100–150 cells were measured for each data point).

two parallel broad laser beams (>5 mm each in diameter, 532 and 1,064 nm) in single pulse mode, (iii) matching the pulse repetition rate (10 Hz and higher) to the cell flow to expose every flowing cell to both laser pulses and at the same time to avoid double exposure. For the cell concentration typical for current methods (up to 10^7 cell/ml), the system can process more than 100 mln cells per minute so that a 10-minute processing yields up to above 1 billion cells, a sufficient amount to infuse to a patient for cell and gene therapy (assuming a high transfection and recovery rate of CD3+ cells and low residual level of CD25+ cells). The latter end points were measured for the gold-laser treatment parameters determined in static mode. The cells were incubated for 1 hour with gold conjugates, and then the plasmid was added to the cell suspension. Then we processed cell suspensions in the PNB flow system using a sterile contour "source syringe-cuvette-collecting syringe" (Figure 1c,d). The laser beams of 1,064 and 532 nm illuminated the cuvette with a small spatial gap so that the flowing cells were first exposed to 532 nm pulse at 65 mJ/cm^2 and then to 1,064 nm pulse at 65 mJ/cm^2. Flow rate and the pulse repetition rate provided that each cell was exposed to a single 532 nm pulse and then to a single 1,064 nm pulse. The source and collecting syringes were operated by two synchronized syringe pumps. The PNB generation in gold-treated cells was additionally verified by exposing individual cells in aliquots of each cell population to single laser pulses of identical fluence and wavelength to those in the flow PNB system. In this experiment, PNB lifetimes coincided with those observed in the static experiments described above (Figure 5).

After a single flow processing of CD3+ and CD25+ cells with identical laser parameters, we observed 77 ± 18% transfection efficacy of CD3+ cells with their 95% effective cell viability (measured 4 days after processing relative to the viability of unprocessed control population of the same cells; the effective cell viability was also measured 10 minutes after treatment and was found to be 96%) and 99.4% efficacy of elimination of CD25+ cells (Table 1). The cells without gold conjugate pre-treatment yielded levels of transfection of CD3+ cells and destruction of CD25+ cells comparable to those of untreated intact (control) cells. Thus, transfection of CD3+ and elimination of CD25+ cells were achieved only through the generation of cell-specific PNBs.

Table 1 Efficacy of transfection and destruction of specific cells

	Level of transfected cells		*Level of destructed cells (based upon the measurement of effective cell viability)*	
	Standard (electroporation)	*PNB*	*Standard (electroporation)*	*PNB*
Transfection target—CD3+ cells				
Control	3.0 ± 3.0	2.5 ± 2.5	1.5 ± 0.5	3.0 ± 2.0
Test	12.0 ± 5.0	77.0 ± 18.0	40.0 ± 3.0	5.0 ± 2.0
Destruction target—CD25+ cells				
Control	n/a	n/a	n/a	0.7 ± 0.4
Test	n/a	n/a	n/a	99.4 ± 0.4

PNB, plasmonic nanobubbles.

Comparison of the PNB technology with standard electroporation (CD3+ cells)

To compare the performance of PNB flow technology to standard cell processing techniques, the same amount of CD3+ cells was transfected via electroporation using the Amaxa Nucleofector system. The efficacy and safety of standard method was lower than those of the PNB technology. Electroporation efficacy was almost 6.5-fold lower and cell recovery for CD3+ cells was 1.5-fold lower. The total time to use the standard techniques for transfection and separation of the similar amount of cells was more than 20-fold longer compared to the PNB flow technology.

DISCUSSION

Comparison to current and investigational technologies

The results obtained demonstrate the high efficacy of the PNB technology for transfection of CD3+ cells and elimination of unwanted CD25+ cells. However, the main advantage is a simultaneous two-in-one functionality of the transfection and elimination of heterogeneous cell system with the high target cell specificity. The multi-functionality is unique for the PNB technology due to entirely new mechanism of action, nonstationary physical (mechanical) intracellular nanoevent (PNB). This is a nonstationary nanoscale transient nature of the cell transfection and destruction that provides high specificity and efficacy of these basic cell processing functions. In contrast, current approaches treat all exposed cells equally on a macro-scale and thus cannot provide the target cell specificity in heterogeneous cell systems. Nonstationary nature and nano-scale of the PNB events employed provide the single cell mechanisms during the bulk treatment of many cells with a broad laser pulse. This allows for the high processing rate, which cannot be achieved with other single cell-based methods, such as flow cytometry or microscopy-based cell processing methods, which operate on a cell-by-cell basis and cannot achieve the PNB cell processing rate (> 10^8 cell/minute).

PNB technology is principally different from current laser-based methods of cell processing. Such methods in gene transfection[44] employ heating,[45] shockwave generation,[25] optical breakdown,[27,29,30] and macro-bubble generation.[28–30] The latter bubbles originate from external thermal or cavitation sources, have macro extracellual nature and thus they cannot discriminate target from nontarget cells. Thus, no current laser methods provide target cell specificty in heterogenous cell systems. Moreover, almost all external energy-based methods depend on the slow diffusion of plasmids through an entry point produced in the cell membrane. Rapid active delivery through opto-injection can be achieved only by individually treating specific single cells by focusing pulsed laser beam on individual cells and activating optical breakdown.[27,29,30] Such laser methods require precise pointing of the focused laser beam on an individual target cell and therefore cannot be used for bulk treatment with high processing rates the PNB technology provides. Compared to current gold nanoparticle-based laser methods of gene delivery and photothermal destruction of cells,[37–42,61–64] PNB technology uses much lower doses of gold nanoparticles and laser energy, three to six orders of magnitude the above cited approaches. Thus, the PNB technology developed here has demonstrated several innovative features: (i) Dual functionality of transfection/elimination in all-in-one simultaneous procedure; (ii) High processing rate of 100 million cell/min which can deliver a therapeutic number of cells in a few minutes, (iii) single target cell specificity in heterogeneous cell system, and (iv) this technology (and PNBs in general) successfully transfected human cells with a potentially therapeutic gene.

Applications and safety for patients

The high precision of the PNB cell processing technology suggests it would be appropriate for broad clinical applications including (i) gene and cell therapy, (ii) bone marrow transplantation,[56,59] and (iii) engineering of stem cells. As for the safety for patient, gold nanoparticles alone are the safest exogenous materials among all available. Our current and past experiments did not show any cytotoxicity or *in vivo* toxicity of gold.[48–60,65] This is because we use low doses, and the amount of gold remaining in cells being transfused to a patient is negligible. In clinic, much higher doses of gold were shown to be safe.[66–69]

Conclusions

The developed novel PNB cell processing technology has been tested in human T-cells and demonstrated the following unprecedented performance:

1. Simultaneous transfection of CD3+ cells and elimination of CD25+ cells with high target cell specificity in all-in-one procedure.
2. A combination of high efficacy (77 ± 18%) and safety (95% recovered) of the cell transfection with the therapeutic gene with high efficacy of the elimination of unwanted cells (99%) and high speed of cell processing, 100 mln cells per minute.
3. The universal physical mechanisms and simple technical design of the PNB flow technology will support its efficient translation to clinic for a broad range of applications which include *ex vivo* processing of cell systems.

MATERIALS AND METHODS

Cells

T lymphocytes were isolated from cord blood (MD Anderson Cord Blood Bank) by flow cytometric cell sorting (Becton Dickinson FACS Aria II) in The Flow Cytometry and Cellular Imaging Core Facility of the University of Texas MD Anderson Cancer Center. A homogeneous samples of viable T-reg were obtained with the BD Pharmingen brand Human Regulatory T Cell Cocktail Kit.

Gold nanoparticles

Conjugation with targeting antibodies. Two types of GNPs were used in this work: 60 nm gold spheres (NSP60) obtained from VanPelt Biosciences LLC (Montgomery Village, MD) and 240 nm solid silica-gold shells (NS240) obtained from NanoComposix (San Diego, CA). The optical absorption maximum of the 60-nm gold spheres is close to 532 and of 240 nm nanoshells is close to 1,064 nm. For active targeting and endocytosis, the GNPs were covalently conjugated to CD3 and to CD25 antibodies by VanPelt Biosciences LLC (Montgomery Village, MD). Both NP conjugates were stored in 0.1× PBS and 0.5% (w/v) BSA. The latter prevented a spontaneous clustering of GNPs in solution.

Targeting: incubation with the cells. CD3-positive T-cells were targeted with covalently conjugates NSP60-CD3. Cells ($2*10^6$ cell/ml) were resuspended in a serum-free RPMI-1640 medium (Invitrogen, Grand Island, NY) containing GNPs at a concentration of 10^{10} particles/ml and incubated with the GNP-containing media for 1 hour at 37 °C in a CO_2 incubator. Following incubation, the cells were washed twice to remove unbound GNPs and finally suspended in RPMI-1640 medium supplemented with serum and antibiotics. The same incubation procedure was applied to targeting the CD25-positive T-reg cells with covalently conjugates NS240-CD25.

Molecular cargo injection

Fluorescence dye FITC-Dextran (2 mg/ml, molecular weight 2 MDa) was used for modelling the injection of the external molecular cargo into the CD3-positive cells. For that the dye was added to the sample of the CD3-positive cells just prior to their exposure to laser pulses and was washed three times with fresh media after the PNB generation. Previously we have found that optical absorption of the laser pulse by FITC-Dextran in cells is not influence the PNB generation.[54] The cell concentration and viability (by Trypan Blue test) was tested before and 10 minutes after the PNB treatment of cell suspensions. The individual living cells were assayed with a laser confocal microscopy (LSM-710, Carl Zeiss MicroImaging GmbH, Germany) in bright field and fluorescent modes for analyzing the efficacy of the dye injection.

To measure the safety of the cell treatment, we applied two independent techniques:

- The cell viability was measured with Trypan Blue test;
- The cell concentration was measured through the cell counts.

In our study, we applied one complex metric that combined the changes in cell concentration and viability, defined as the effective cell viability (*RV*) and calculated as a product of the cell viability and concentration:

$$RV = C_t/C_0*V*100\%,$$

where C_t is cell concentration after treatment, C_0 is the cell concentration in untreated control, and *V* is the viability of the cells measured after PNB treatment. The cell concentration was identical in all samples before treatment. In addition, we monitored the shape and structure of the cells before and after PNB treatment though their imaging with the microscope CDD camera (Andor Luca EMCCD, Belfast, UK). Thus, three independent methodologies were employed to monitor the cells during the PNB treatment.

Gene transfection

Engineered T cells with safety switches have been developed to increase the feasibility of infusing potentially therapeutic cell numbers while providing a tool to control any adverse events due to T-cell activation and expansion. As our gene of interest, therefore, we used an inducible human caspase 9 transgene (iC9) the product of which is dimerized, and hence activated, by administration of an otherwise bio-inert small molecule drug, AP1903, thereby rapidly inducing apoptosis in the transduced cells. In the experiments with the transfection of CD3-positive cells, we added the pMSCV-F-del Casp9. IRES.GFP plasmid into the cells suspension in the concentration of 50 μg/ml and was washed three times with fresh media immediately after the PNB generation. pMSCV-F-del Casp9.IRES.GFP was a gift from David Spencer (Addgene plasmid # 15567). After PNB-treatment, cells were placed in an incubator under standard cultivation conditions and GFP-fluorescence and effective cell viability were analyzed at 0, 48, 72, and 96 hours. GFP-fluorescence was tested in the individual cells with laser confocal microscopy (LSM-710, Carl Zeiss MicroImaging GmbH, Germany) in bright field and fluorescent (100–150 cells were tested in each sample). An addition, the effective cell viability was measured 10 minutes after PNB treatment of the cells.

PNB generation and detection

A PNB is a vapor nanobubble transiently induced around a superheated intracellular gold NP cluster upon absorption of a short laser pulse. Gold nanoparticles (GNPs) convert optical energy into heat through the mechanism of plasmon resonance[46,47] and evaporate the surrounding liquid. To avoid thermal losses and to minimize optical doses, we apply single short (20–25 ps) (Ekspla, Vilnius, Lithuania) pulses at the wavelength of the maximal efficacy of PNB generation, visible or near-infrared.[70–72] The biological function of a PNB is determined by its maximal size that is measured through the PNB lifetime.[47] Small PNBs of 50–100 ns provide efficient noninvasive gene transfer by injecting external plasmid[51,53] (Figure 1a). Larger PNBs of > 200 ns lifetime efficiently destroy cells[54–58] (Figure 1b).

Unlike many other photoinduced events such as heat, sound, or light, a PNB has a generation threshold fluence that is sensitive to clustering of GNPs.[47–60,65] The PNB generation threshold fluence was found to decrease with the GNP cluster size, so it is the lowest for the largest GNP clusters in target cells and the highest for single GNPs nonspecifically internalized by nontarget cells.[48,50,60] This unique physical property of PNBs results in an unprecedented cellular specificity due to: (i) the threshold mechanism of PNB generation, (ii) the dependence of the PNB generation threshold fluence upon the size of the GNP cluster, and (iii) target cell-specific formation of the largest GNP clusters through receptor-mediated endocytosis.[48–50] The cellular specificity of PNBs was found to be more than one order of magnitude higher than that of GNPs in the mixed cell models

To detect the PNBs, we used an optical scattering method developed by us earlier.[46,47,73] This method measures the PNB lifetime (characterizing the maximal diameter of a PNB[46,47,73] in individual cells. In addition, we used a low power probe laser to detect the optical scattering signals of PNBs as

time-resolved images and time-response (Figure 2a). The combination of the NP parameters and of the laser wavelength and fluence were optimized to achieve a PNB lifetime of 70–90 ns in CD3+ cells, 200–300 ns in T-reg cells. For that purpose, we used our photothermal microscope.[46,47,73]

Cell transfection and destruction with PNBs

Gene transfer with PNBs (Figure 1) was achieved by generating small PNBs with a lifetime of 70–80 ns in CD3+ T-cells. We used with NSP60-CD3 (T-cell specific) antibody conjugates to selectively form NSP clusters in CD3+ T-cells that generated relatively small PNBs. The mechanism of the delivery of plasmids includes: (i) creating a transient hole in the cellular membrane due to the localized explosive effect of a PNB, (ii) injecting extracellular plasmid molecules into the cytoplasm with a PNB-induced nanojet.

A large PNB (>200 ns) mechanically disrupts a cell, causing its immediate and irreversible lysis-like destruction[54–58] (not apoptosis or necrosis). This destruction mechanism acts instantaneously, demonstrates single target cell specificity and negligible nonspecific toxicity.[48–60,65] We developed this method for eliminating T-reg cells without damaging conventional T-cells or nontarget cells in the graft. Since T-reg cells are CD25+, we used NS240-CD25 conjugates to target this sub-set. Under identical optical excitation, NS clusters in CD25+ T-reg cells generated much larger PNBs than NSP clusters in CD3+ T cells), simultaneously inducing two different consequences in T-cells (transfection) and T-reg cells (destruction) under identical exposure to a single pulse.

Standard cell processing: electroporation

The electroporation of CD3+ cells was performed with the Amaxa Nucleofector system (Amaxa Human T cell Nucleofection Kit). For that the cells were resuspended in Nucleofector solution with 50 µg/ml of plasmid and treated with program U-14 according to the manufacturer's instructions. Immediately after that cells were transferred into 500 µl prewarmed media and were additionally washed with fresh media before their culturing.

CONFLICT OF INTEREST

The authors declare no conflict of interest.

ACKNOWLEDGMENTS

Authors thank Malcolm K. Brenner of Center for Cell and Gene Therapy, Baylor College of Medicine, The Methodist Hospital and Texas Children's Hospital, Houston, TX, for the his continuing support of this technology and helpful guidance. This work was supported by the grants from NIH (R21EB017384) and Gillson Langenbaugh Foundation (Houston, TX). The Flow Cytometry and Cellular Imaging Core Facility of the University of Texas MD Anderson Cancer Center is funded by NCI Cancer Center Support Grant P30CA16672.

REFERENCES

1. Tricot, G, Gazitt, Y, Leemhuis, T, Jagannath, S, Desikan, KR, Siegel, D *et al*. (1998). Collection, tumor contamination, and engraftment kinetics of highly purified hematopoietic progenitor cells to support high dose therapy in multiple myeloma. *Blood* **91**: 4489–4495.
2. Holmberg, LA, Boeckh, M, Hooper, H, Leisenring, W, Rowley, S, Heimfeld, S *et al.* (1999). Increased incidence of cytomegalovirus disease after autologous CD34-selected peripheral blood stem cell transplantation. *Blood* **94**: 4029–4035.
3. Tomlinson, MJ, Tomlinson, S, Yang, XB and Kirkham, J (2013). Cell separation: Terminology and practical considerations. *J Tissue Eng* **4**: 2041731412472690.
4. Almeida, M, García-Montero, AC and Orfao, A (2014). Cell purification: a new challenge for biobanks. *Pathobiology* **81**: 261–275.
5. Orfao, A and Ruiz-Arguelles, A (1996). General concepts about cell sorting techniques. *Clin Biochem* **29**: 5–9.
6. Will, B and Steidl, U (2010). Multi-parameter fluorescence-activated cell sorting and analysis of stem and progenitor cells in myeloid malignancies. *Best Pract Res Clin Haematol* **23**: 391–401.
7. Handgretinger, R, Lang, P, Schumm, M, Taylor, G, Neu, S, Koscielnak, E *et al.* (1998). Isolation and transplantation of autologous peripheral CD34+ progenitor cells highly purified by magnetic-activated cell sorting. *Bone Marrow Transplant* **21**: 987–993.
8. Al-Mawali, A, Gillis, D and Lewis, I (2009). The role of multiparameter flow cytometry for detection of minimal residual disease in acute myeloid leukemia. *Am J Clin Pathol* **131**: 16–26.
9. Cazzaniga, G, Gaipa, G, Rossi, V and Biondi, A (2006). Monitoring of minimal residual disease in leukemia, advantages and pitfalls. *Ann Med* **38**: 512–521.
10. Rawstron, AC, Orfao, A, Beksac, M, Bezdickova, L, Brooimans, RA, Bumbea, H *et al.*; European Myeloma Network. (2008). Report of the European Myeloma Network on multiparametric flow cytometry in multiple myeloma and related disorders. *Haematologica* **93**: 431–438.
11. van der Velden, VH, Hochhaus, A, Cazzaniga, G, Szczepanski, T, Gabert, J and van Dongen, JJ (2003). Detection of minimal residual disease in hematologic malignancies by real-time quantitative PCR: principles, approaches, and laboratory aspects. *Leukemia* **17**: 1013–1034.
12. Rutella, S, Rumi, C, Laurenti, L, Pierelli, L, Sora', F, Sica, S *et al.* (2000). Immune reconstitution after transplantation of autologous peripheral CD34+ cells: analysis of predictive factors and comparison with unselected progenitor transplants. *Br J Haematol* **108**: 105–115.
13. Pfeifer, A and Verma, IM (2001). Gene therapy: promises and problems. *Annu Rev Genomics Hum Genet* **2**: 177–211.
14. Kreppel, F and Kochanek, S (2008). Modification of adenovirus gene transfer vectors with synthetic polymers: a scientific review and technical guide. *Mol Ther* **16**: 16–29.
15. Kim, TK and Eberwine, JH (2010). Mammalian cell transfection: the present and the future. *Anal Bioanal Chem* **397**: 3173–3178.
16. Rogers, ML and Rush, RA (2012). Non-viral gene therapy for neurological diseases, with an emphasis on targeted gene delivery. *J Control Release* **157**: 183–189.
17. O'Neill, MM, Kennedy, CA, Barton, RW and Tatake, RJ (2001). Receptor-mediated gene delivery to human peripheral blood mononuclear cells using anti-CD3 antibody coupled to polyethylenimine. *Gene Ther* **8**: 362–368.
18. Mars, T, Strazisar, M, Mis, K, Kotnik, N, Pegan, K, Lojk, J *et al.* (2015). Electrotransfection and lipofection show comparable efficiency for *in vitro* gene delivery of primary human myoblasts. *J Membr Biol* **248**: 273–283.
19. Arima, H, Chihara, Y, Arizono, M, Yamashita, S, Wada, K, Hirayama, F *et al.* (2006). Enhancement of gene transfer activity mediated by mannosylated dendrimer/alpha-cyclodextrin conjugate (generation 3, G3). *J Control Release* **116**: 64–74.
20. Balazs, DA and Godbey, W (2011). Liposomes for use in gene delivery. *J Drug Deliv* **2011**: 326497.
21. Bazan-Peregrino, M, Arvanitis, CD, Rifai, B, Seymour, LW and Coussios, CC (2012). Ultrasound-induced cavitation enhances the delivery and therapeutic efficacy of an oncolytic virus in an *in vitro* model. *J Control Release* **157**: 235–242.
22. Lee, S, McAuliffe, DJ, Flotte, TJ, Kollias, N and Doukas, AG (1998). Photomechanical transcutaneous delivery of macromolecules. *J Invest Dermatol* **111**: 925–929.
23. Qiu, Y, Luo, Y, Zhang, Y, Cui, W, Zhang, D, Wu, J *et al.* (2010). The correlation between acoustic cavitation and sonoporation involved in ultrasound-mediated DNA transfection with polyethylenimine (PEI) *in vitro*. *J Control Release* **145**: 40–48.
24. Choi, Y, Yuen, C, Maiti, SN, Olivares, S, Gibbons, H, Huls, H *et al.* (2010). A high throughput microelectroporation device to introduce a chimeric antigen receptor to redirect the specificity of human T cells. *Biomed Microdevices* **12**: 855–863.
25. Schomaker, M, Baumgart, J, Ngezahayo, A, Bullerdiek, J, Nolte, I, Escobar, HM, *et al.* (2009) Plasmonic perforation of living cells using ultrashort laser pulses and gold nanoparticles. *SPIE Proc* **7192**: 71920U.
26. Soughayer, JS, Krasieva, T, Jacobson, SC, Ramsey, JM, Tromberg, BJ and Allbritton, NL (2000). Characterization of cellular optoporation with distance. *Anal Chem* **72**: 1342–1347.
27. Stevenson, D, Agate, B, Tsampoula, X, Fischer, P, Brown, CT, Sibbett, W *et al.* (2006). Femtosecond optical transfection of cells: viability and efficiency. *Opt Express* **14**: 7125–7133.
28. Arita, Y, Torres-Mapa, ML, Lee, WM, Cizmar, T, Campbell, P, Gunn-Moore, FJ, *et al.* (2011) Spatially optimized gene transfection by laser-induced breakdown of optically trapped nanoparticles. *Appl Phys Lett* **98**: 093702.
29. Baumgart, J, Bintig, W, Ngezahayo, A, Willenbrock, S, Murua Escobar, H, Ertmer, W *et al.* (2008). Quantified femtosecond laser based opto-perforation of living GFSHR-17 and MTH53 a cells. *Opt Express* **16**: 3021–3031.
30. Kohli, V, Acker, JP and Elezzabi, AY (2005). Reversible permeabilization using high-intensity femtosecond laser pulses: applications to biopreservation. *Biotechnol Bioeng* **92**: 889–899.
31. Felgner, PL, Gadek, TR, Holm, M, Roman, R, Chan, HW, Wenz, M *et al.* (1987). Lipofection: a highly efficient, lipid-mediated DNA-transfection procedure. *Proc Natl Acad Sci USA* **84**: 7413–7417.
32. Hedrich, CM, Rauen, T, Kis-Toth, K, Kyttaris, VC and Tsokos, GC (2012). cAMP-responsive element modulator α (CREMα) suppresses IL-17F protein expression in T lymphocytes from patients with systemic lupus erythematosus (SLE). *J Biol Chem* **287**: 4715–4725.
33. Yang, S, Gattinoni, L, Luca, G, Liu, F, Ji, Y, Yu, Z *et al.* (2011). *In vitro* generated anti-tumor T lymphocytes exhibit distinct subsets mimicking *in vivo* antigen-experienced cells. *Cancer Immunol Immunother* **60**: 739–749.
34. Shukla, S, Kavak, E, Gregory, M, Imashimizu, M, Shutinoski, B, Kashlev, M *et al.* (2011). CTCF-promoted RNA polymerase II pausing links DNA methylation to splicing. *Nature* **479**: 74–79.

35. Curtale, G, Citarella, F, Carissimi, C, Goldoni, M, Carucci, N, Fulci, V *et al.* (2010). An emerging player in the adaptive immune response: microRNA-146a is a modulator of IL-2 expression and activation-induced cell death in T lymphocytes. *Blood* **115**: 265–273.
36. Sarhan, MA, Pham, TN, Chen, AY and Michalak, TI (2012). Hepatitis C virus infection of human T lymphocytes is mediated by CD5. *J Virol* **86**: 3723–3735.
37. Gaspar, VM, Correia, IJ, Sousa, A, Silva, F, Paquete, CM, Queiroz, JA *et al.* (2011). Nanoparticle mediated delivery of pure P53 supercoiled plasmid DNA for gene therapy. *J Control Release* **156**: 212–222.
38. Pissuwan, D, Niidome, T and Cortie, MB (2011). The forthcoming applications of gold nanoparticles in drug and gene delivery systems. *J Control Release* **149**: 65–71.
39. Jain, PK, Huang, X, El-Sayed, IH and El-Sayed, MA (2008). Noble metals on the nanoscale: optical and photothermal properties and some applications in imaging, sensing, biology, and medicine. *Acc Chem Res* **41**: 1578–1586.
40. Braun, GB, Pallaoro, A, Wu, G, Missirlis, D, Zasadzinski, JA, Tirrell, M *et al.* (2009). Laser-Activated Gene Silencing via Gold Nanoshell-siRNA Conjugates. *ACS Nano* **3**: 2007–2015.
41. Baldi, L, Hacker, DL, Meerschman, C and Wurm, FM (2012) Large-scale transfection of mammalian cells. *Methods Mol Biol* **801**: 13–26.
42. Song, J, Cheng, L, Liu, A, Yin, J, Kuang, M and Duan, H (2011). Plasmonic vesicles of amphiphilic gold nanocrystals: self-assembly and external-stimuli-triggered destruction. *J Am Chem Soc* **133**: 10760–10763.
43. Kurosawa, A, Saito, S, Mori, M and Adachi, N (2012). Nucleofection-based gene targeting in human pre-B cells. *Gene* **492**: 305–308.
44. Tsukakoshi, M, Kurata, S, Nomiya, Y, Ikawa, Y, Kasuya, T (1984). A novel method of DNA transfection by laser microbeam cell surgery. *Appl Phys B-Photo* **35**: 135–140.
45. Palumbo, G, Caruso, M, Crescenzi, E, Tecce, MF, Roberti, G and Colasanti, A (1996). Targeted gene transfer in eucaryotic cells by dye-assisted laser optoporation. *J Photochem Photobiol B* **36**: 41–46.
46. Lukianova-Hleb, EY and Lapotko, DO (2009). Influence of transient environmental photothermal effects on optical scattering by gold nanoparticles. *Nano Lett* **9**: 2160–2166.
47. Lukianova-Hleb, E, Hu, Y, Latterini, L, Tarpani, L, Lee, S, Drezek, RA *et al.* (2010). Plasmonic nanobubbles as transient vapor nanobubbles generated around plasmonic nanoparticles. *ACS Nano* **4**: 2109–2123.
48. Wagner, DS, Delk, NA, Lukianova-Hleb, EY, Hafner, JH, Farach-Carson, MC and Lapotko, DO (2010). The *in vivo* performance of plasmonic nanobubbles as cell theranostic agents in zebrafish hosting prostate cancer xenografts. *Biomaterials* **31**: 7567–7574.
49. Lapotko, D (2011). Plasmonic nanobubbles as tunable cellular probes for cancer theranostics. *Cancers (Basel)* **3**: 802–840.
50. Lukianova-Hleb, EY, Ren, X, Constantinou, PE, Danysh, BP, Shenefelt, DL, Carson, DD *et al.* (2012). Improved cellular specificity of plasmonic nanobubbles versus nanoparticles in heterogeneous cell systems. *PLoS One* **7**: e34537.
51. Lukianova-Hleb, EY, Samaniego, AP, Wen, J, Metelitsa, LS, Chang, CC and Lapotko, DO (2011). Selective gene transfection of individual cells *in vitro* with plasmonic nanobubbles. *J Control Release* **152**: 286–293.
52. Lukianova-Hleb, EY, Ren, X, Zasadzinski, JA, Wu, X and Lapotko, DO (2012). Plasmonic nanobubbles enhance efficacy and selectivity of chemotherapy against drug-resistant cancer cells. *Adv Mater* **24**: 3831–3837.
53. Lukianova-Hleb, EY, Wagner, DS, Brenner, MK and Lapotko, DO (2012). Cell-specific transmembrane injection of molecular cargo with gold nanoparticle-generated transient plasmonic nanobubbles. *Biomaterials* **33**: 5441–5450.
54. Lukianova-Hleb, EY, Mutonga, MB and Lapotko, DO (2012). Cell-specific multifunctional processing of heterogeneous cell systems in a single laser pulse treatment. *ACS Nano* **6**: 10973–10981.
55. Hleb, EY, Hafner, JH, Myers, JN, Hanna, EY, Rostro, BC, Zhdanok, SA *et al.* (2008). LANTCET: elimination of solid tumor cells with photothermal bubbles generated around clusters of gold nanoparticles. *Nanomedicine (Lond)* **3**: 647–667.
56. Lapotko, D, Lukianova, E, Potapnev, M, Aleinikova, O and Oraevsky, A (2006). Method of laser activated nano-thermolysis for elimination of tumor cells. *Cancer Lett* **239**: 36–45.
57. Lukianova-Hleb, EY, Koneva, II, Oginsky, AO, La Francesca, S and Lapotko, DO (2011). Selective and self-guided micro-ablation of tissue with plasmonic nanobubbles. *J Surg Res* **166**: e3–13.
58. Lukianova-Hleb, E, Hanna, EY, Hafner, JH, Lapotko, DO (2010). Tunable plasmonic nanobubbles for cell theranostics. *Nanotechnology* **21**: 085102.
59. Lapotko, DO, Lukianova, E and Oraevsky, AA (2006). Selective laser nano-thermolysis of human leukemia cells with microbubbles generated around clusters of gold nanoparticles. *Lasers Surg Med* **38**: 631–642.
60. Lukianova-Hleb, EY, Ren, X, Sawant, RR, Wu, X, Torchilin, VP and Lapotko, DO (2014). On-demand intracellular amplification of chemoradiation with cancer-specific plasmonic nanobubbles. *Nat Med* **20**: 778–784.
61. Wang, F, Wang, YC, Dou, S, Xiong, MH, Sun, TM and Wang, J (2011). Doxorubicin-tethered responsive gold nanoparticles facilitate intracellular drug delivery for overcoming multidrug resistance in cancer cells. *ACS Nano* **5**: 3679–3692.
62. Kim, B, Han, G, Toley, BJ, Kim, CK, Rotello, VM and Forbes, NS (2010). Tuning payload delivery in tumour cylindroids using gold nanoparticles. *Nat Nanotechnol* **5**: 465–472.
63. Rai, P, Mallidi, S, Zheng, X, Rahmanzadeh, R, Mir, Y, Elrington, S *et al.* (2010). Development and applications of photo-triggered theranostic agents. *Adv Drug Deliv Rev* **62**: 1094–1124.
64. Zhang, Z, Wang, L, Wang, J, Jiang, X, Li, X, Hu, Z *et al.* (2012). Mesoporous silica-coated gold nanorods as a light-mediated multifunctional theranostic platform for cancer treatment. *Adv Mater* **24**: 1418–1423.
65. Lukianova-Hleb, EY, Ren, X, Townley, D, Wu, X, Kupferman, ME and Lapotko, DO (2012). Plasmonic nanobubbles rapidly detect and destroy drug-resistant tumors. *Theranostics* **2**: 976–987.
66. Libutti, SK, Paciotti, GF, Byrnes, AA, Alexander, HR Jr, Gannon, WE, Walker, M *et al.* (2010). Phase I and pharmacokinetic studies of CYT-6091, a novel PEGylated colloidal gold-rhTNF nanomedicine. *Clin Cancer Res* **16**: 6139–6149.
67. Merchant, B (1998). Gold, the noble metal and the paradoxes of its toxicology. *Biologicals* **26**: 49–59.
68. Root, SW, Andrews, GA, Kniseley, RM and Tyor, MP (1954). The distribution and radiation effects of intravenously administered colloidal Au198 in man. *Cancer* **7**: 856–866.
69. Kean, WF and Kean, IR (2008). Clinical pharmacology of gold. *Inflammopharmacology* **16**: 112–125.
70. Lukianova-Hleb, EY, Sassaroli, E, Jones, A and Lapotko, DO (2012). Transient photothermal spectra of plasmonic nanobubbles. *Langmuir* **28**: 4858–4866.
71. Lukianova-Hleb, EY, Volkov, AN, Wu, X and Lapotko, DO (2013). Transient enhancement and spectral narrowing of the photothermal effect of plasmonic nanoparticles under pulsed excitation. *Adv Mater* **25**: 772–776.
72. Lukianova-Hleb, EY, Volkov, AN and Lapotko, DO (2014). Laser pulse duration is critical for the generation of plasmonic nanobubbles. *Langmuir* **30**: 7425–7434.
73. Lapotko, D (2009). Optical excitation and detection of vapor bubbles around plasmonic nanoparticles. *Opt Express* **17**: 2538–2556.